nature medicine

Neural precursor cells induce cell death of high-grade astrocytomas through stimulation of TRPV1

Kristin Stock[1,16], Jitender Kumar[1,16], Michael Synowitz[1,2,16], Stefania Petrosino[3], Roberta Imperatore[4], Ewan St J Smith[5,6], Peter Wend[7,15], Bettina Purfürst[8], Ulrike A Nuber[9], Ulf Gurok[10], Vitali Matyash[1], Joo-Hee Wälzlein[1], Sridhar R Chirasani[1], Gunnar Dittmar[11], Benjamin F Cravatt[12], Stefan Momma[13], Gary R Lewin[5], Alessia Ligresti[3], Luciano De Petrocellis[4], Luigia Cristino[4], Vincenzo Di Marzo[3], Helmut Kettenmann[1,16] & Rainer Glass[1,14,16]

Primary astrocytomas of grade 3 or 4 according to the classification system of the World Health Organization (high-grade astrocytomas or HGAs) are preponderant among adults and are almost invariably fatal despite the use of multimodal therapy. Here we show that the juvenile brain has an endogenous defense mechanism against HGAs. Neural precursor cells (NPCs) migrate to HGAs, reduce glioma expansion and prolong survival time by releasing endovanilloids that activate the vanilloid receptor (transient receptor potential vanilloid subfamily member-1 or TRPV1) on HGA cells. TRPV1 is highly expressed in tumor and weakly expressed in tumor-free brain. TRPV1 stimulation triggers tumor cell death through the branch of the endoplasmic reticulum stress pathway that is controlled by activating transcription factor-3 (ATF3). The antitumorigenic response of NPCs is lost with aging. NPC-mediated tumor suppression can be mimicked in the adult brain by systemic administration of the synthetic vanilloid arvanil, suggesting that TRPV1 agonists have potential as new HGA therapeutics.

Somatic mutant neural stem cells and NPCs are thought to be the source of HGAs, one of the most aggressive forms of tumors of the central nervous system (CNS)[1]. A very large fraction of individuals diagnosed with HGAs and glioblastomas (GBMs) are adults[2,3]. However, adult neurogenesis (that is, the presence and activity of NPCs in the postnatal and adult brain) is maintained at a high rate only during infancy and declines thereafter[4,5]. Hence, the epidemiology of GBMs and the timing of adult neurogenesis are inversely correlated, and GBMs are often diagnosed several decades after the decline in brain stem cell activity.

It has been previously found that endogenous and exogenous NPCs have a strong tropism for primary brain tumors and that NPCs can release tumor-suppressive factors[6–13]. However, the molecular nature of the factors that mediate cell death in HGA cells has not been elucidated. We show that NPCs induce tumor cell death through the release of endovanilloids. Endovanilloids[14], such as arachidonoyl ethanolamide (AEA) and *N*-arachidonoyl dopamine (NADA), directly stimulate the vanilloid receptor, TRPV1, which is abundantly expressed on HGA[15]. TRPV1 is a nonselective cation channel that is best characterized in capsaicin-sensitive sensory neurons of the dorsal root and trigeminal ganglia[16]. Synergistic TRPV1 activation by AEA in combination with other fatty acid ethanolamides, such as oleoyl ethanolamide (OEA) or palmitoyl ethanolamide (PEA), has previously been reported[15,16]. The physiological role of the ion channel in non-neural tissues is largely unexplored[16]. Here we show that endovanilloid release from NPCs activates TRPV1 on HGA cells and thereby induces tumor-cell death.

RESULTS

NPCs induce HGA cell death through TRPV1

We investigated the signaling pathways that are activated in HGA cells after exposure to NPC-conditioned medium (NPC-CM). An analysis of gene expression changes (by microarrays of stimulated and control HGA cells; GSE37671) together with pharmacological studies using specific TRPV1 antagonists and molecular studies using specific TRPV1 knockdown in HGA cells suggested a role for NPC-derived endovanilloids as tumor suppressors. Furthermore, we observed by real time PCR that TRPV1 expression is positively correlated with grading in human primary brain tumors and that TRPV1 expression in tumors was higher than in human tumor-free brain (**Supplementary Fig. 1a**).

[1]Cellular Neuroscience, Max Delbrück Centre for Molecular Medicine (MDC), Berlin, Germany. [2]Department of Neurosurgery, Charité, University Medicine Berlin, Berlin, Germany. [3]Endocannabinoid Research Group, Institute of Biomolecular Chemistry, Consiglio Nazionale delle Ricerche, Pozzuoli, Italy. [4]Endocannabinoid Research Group, Institute of Cybernetics, Consiglio Nazionale delle Ricerche, Pozzuoli, Italy. [5]Molecular Physiology of Somatic Sensation, MDC, Berlin, Germany. [6]Skirball Institute of Biomolecular Medicine, New York University Langone Medical Center, New York, New York, USA. [7]Signal Transduction, Epithelial Differentiation, Invasion and Metastasis, MDC, Berlin, Germany. [8]Central Facility for Electron Microscopy, MDC, Berlin, Germany. [9]Lund Center for Stem Cell Biology and Cell Therapy, Lund University, Lund, Sweden. [10]Max Planck Institute for Molecular Genetics, Berlin, Germany. [11]Central Facility for Mass Spectrometry, MDC, Berlin, Germany. [12]The Scripps Research Institute, La Jolla, California, USA. [13]Restorative Neurology, Institute of Neurology (Edinger-Institute), Johann Wolfgang Goethe-University Frankfurt, Frankfurt, Germany. [14]Neurosurgical Research, Clinic for Neurosurgery, Ludwig Maximilians University of Munich, Munich, Germany. [15]Present address: David Geffen School of Medicine and Jonsson Comprehensive Cancer Center, University of California at Los Angeles, Los Angeles, California, USA. [16]These authors contributed equally to this work. Correspondence should be addressed to R.G. (rainer.glass@med.uni-muenchen.de).

Received 12 November 2010; accepted 7 May 2012; published online 22 July 2012; doi:10.1038/nm.2827

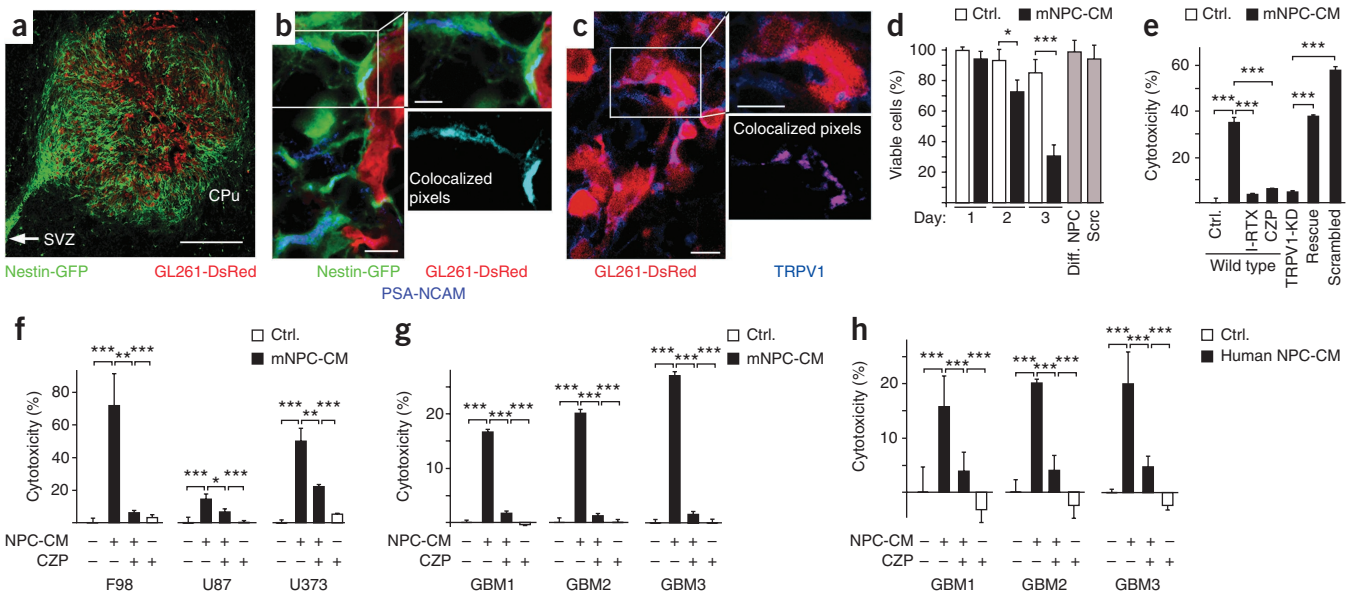

Figure 1 TRPV1 agonists released from NPCs induce HGA cell death. (**a**) Large numbers of nestin-GFP$^+$ cells are present after 14 d of tumor development at a DsRed$^+$ glioma in the caudate putamen (CPu) of young mice (tumor implantation on postnatal day 30; $n = 12$, containing male and female mice for each immunohistochemistry). The arrow points to the subventricular zone (SVZ). Scale bar, 500 µm. (**b**) Glioma-associated nestin-GFP$^+$ cells express PSA-NCAM (blue). A single cell (within the boxed area in the image on the left) is magnified on the right, and colocalizing pixels of a single optical section are shown. Scale bar, left image, 10 µm; magnified image, 6 µm. (**c**) Glioma cells are immunopositive for TRPV1 (blue). A single cell (within the boxed area in the image on the left) is magnified on the right, and colocalizing pixels of a single optical section are shown. Scale bars, 10 µm. (**d**) The viability of mouse GL261 glioma cells is reduced after stimulation with mNPC-CM but not after stimulation with nonconditioned medium (Ctrl.) or other control media (gray bars). Diff. NPC, differentiated NPCs; scrc, nontumorigenic fibroblasts. (**e**) The mNPC-CM–induced cytotoxicity of GL261cells was blocked by CZP and the knockdown of TRPV1 (TRPV1-KD) but not by a control shRNA (scrambled); rescue of the TRPV1-KD fully restored the effect of mNPC-CM. (**f**–**h**) The relative cytotoxicity of primary human GBM cells (**g**,**h**) and HGA cell lines (**f**) after incubation with mNPC-CM (**f**,**g**) or human NPC-CM (**h**) with or without CZP. All data are mean ± s.d. $^*P < 0.05$, $^{**}P < 0.005$, $^{***}P < 0.001$ by Student's t test.

We next explored the role of the endovanilloid system in NPC-mediated HGA suppression in an established mouse model[8,9,17]. We orthotopically implanted brain tumor cells (DsRed-expressing GL261 cells) in nestin-GFP mice, which are a model for the visualization of NPCs[8,18] (**Fig. 1a**). Fourteen days after tumor cell injection, we found that subventricular NPCs migrated to HGAs that were located in the caudate putamen in these mice[8,9,17]. We identified NPCs using colocalization of GFP with established immunocytochemical markers, such as polysialylated neuronal cell adhesion molecule (PSA-NCAM) (**Fig. 1b**) or Musashi[8,19,20]. PSA-NCAM is also a marker of tumor-associated NPCs in humans (S.M., unpublished observations). Notably, we found that the mouse HGAs had higher amounts of immunolabeling for TRPV1 (**Fig. 1c**) than tumor-free brain, whereas only a small fraction of tumor-associated nestin-GFP$^+$ cells expressed TRPV1, and TRPV1 was absent from subventricular NPCs in the mice (**Supplementary Fig. 1b**).

In a series of *in vitro* experiments, we found that stimulation of mouse HGAs with factors released from mouse NPCs (mNPC-CM), but not with factors released from their fully differentiated progeny (astrocytes, oligodendrocytes and neurons) or from fibroblasts (scrc), strongly reduced the viability of HGA cells over a time-course of 3 d (**Fig. 1d**; the data for the conditioned medium from the control cells were obtained on day 3). In subsequent experiments, we stimulated the mouse HGA cells for 3 d, unless indicated otherwise. Stimulation with mNPC-CM reduced the viability of the HGA cells by inducing cell death, as indicated by TUNEL and cytotoxicity assays (**Supplementary Fig. 1c**). All cytotoxicity values are expressed as a percentage of the fully permeabilized cells (**Supplementary Figs. 2** and **3**).

HGAs in the GL261 mouse glioma model express TRPV1 and contain specific binding sites for a selective TRPV1 ligand (**Supplementary Fig. 1d**,**e**). In this model, HGA cell death induced by stimulation with mNPC-CM was greatly reduced by blocking TRPV1 with the selective antagonists[16] iodoresiniferatoxin (I-RTX, 10 nM; **Fig. 1e**) or capsazepine (CZP, 1 µM; **Fig. 1e**) and by knockdown of TRPV1 (TRPV1-KD; **Fig. 1e**). For the knockdown of TRPV1, we expressed five different TRPV1-directed shRNAs and control shRNA (scrambled) in GL261 cells and then selected for vectors that block TRPV1 function in GL261 cells. We subsequently quantified TRPV1 protein expression by quantitative proteomics (selected reaction monitoring, SRM) in knockdown and control GL261 cells (**Supplementary Fig. 1d**). SRM allowed for a direct, specific and well-controlled quantification of TRPV1 protein expression. We verified the efficiency and specificity of the TRPV1 knockdown (**Supplementary Fig. 1d**,**e**) by performing experiments with control shRNAs (scrambled shRNA) and with overexpression of a knockdown-resistant form of mouse TRPV1 (ref. 21) in TRPV1-KD HGA cells (**Fig. 1e**,**f** and **Supplementary Fig. 2c**). Exposure to mNPC-CM strongly induced cell death in various HGA cell lines (**Fig. 1f**) and in three different primary human GBM cultures (**Fig. 1g**), an effect that was blocked by the simultaneous application of either I-RTX (**Supplementary Figs. 2b** and **3a**,**b**) or CZP. Notably, human NPC-CM also induced cell death in primary human GBMs after stimulation of TRPV1 (**Fig. 1h**).

Overall, our cell-culture experiments showed that human and mouse NPCs release TRPV1 agonists, which induce HGA cell death. Our data from a mouse model showed that, in the young brain, many NPCs accumulate at HGAs. An analysis of TRPV1 expression in

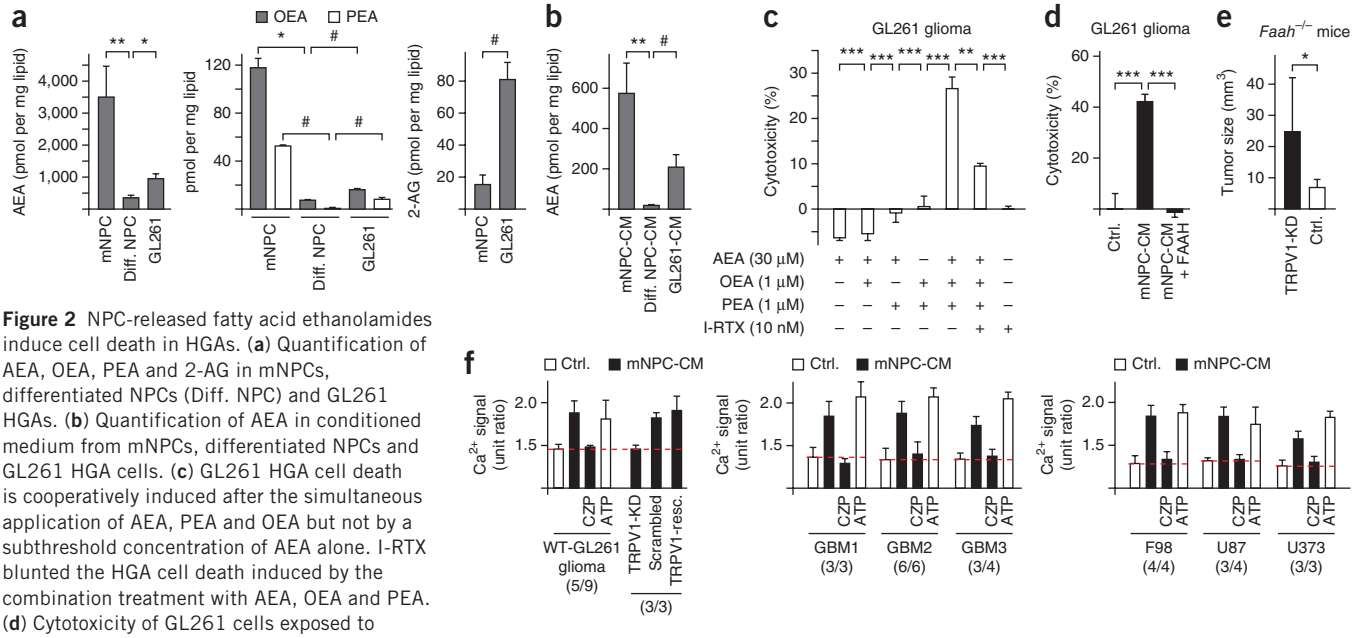

Figure 2 NPC-released fatty acid ethanolamides induce cell death in HGAs. (**a**) Quantification of AEA, OEA, PEA and 2-AG in mNPCs, differentiated NPCs (Diff. NPC) and GL261 HGAs. (**b**) Quantification of AEA in conditioned medium from mNPCs, differentiated NPCs and GL261 HGA cells. (**c**) GL261 HGA cell death is cooperatively induced after the simultaneous application of AEA, PEA and OEA but not by a subthreshold concentration of AEA alone. I-RTX blunted the HGA cell death induced by the combination treatment with AEA, OEA and PEA. (**d**) Cytotoxicity of GL261 cells exposed to nonconditioned medium (Ctrl.), mNPC-CM or mNPC-CM plus FAAH. (**e**) GL261 HGA growth in *Faah*$^{-/-}$ mice with control (Ctrl.) or TRPV1-KD tumors ($n \geq 7$ mice per experimental group, containing male and female mice). (**f**) Ca^{2+} responses in wild-type (WT-GL261), control shRNA (scrambled), TRPV1-KD and TRPV1 rescue GL261 HGA cells (TRPV1-resc.) stimulated with mNPC-CM. Ca^{2+} responses to mNPC-CM were also recorded from three different primary human GBM cultures (middle graph) and HGA cell lines (right graph). CZP blocked the Ca^{2+} signals evoked by mNPC-CM in all cases. The dashed red line indicates the baseline values for each experiment. ATP (1 mM) induced a Ca^{2+} response in all experiments, indicating that all cells were alive and responsive. This figure shows data from representative experiments, and the number of similar experiments out of all experiments is given in parentheses. All data are mean ± s.d. $^{*}P < 0.05$, $^{**}P < 0.005$, $^{***}P < 0.001$ by Fisher's exact test (**a**,**b**) or Student's *t* test (**c**–**e**), and $^{\#}P < 0.001$ by Wilcoxon rank test.

HGAs and tumor-free brain from mice and humans indicated that HGAs have high expression of TRPV1, whereas we found low TRPV1 expression in non-neoplastic CNS.

NPCs constitutively release endovanilloids

We quantified the concentrations of AEA, NADA, OEA, PEA and the endocannabinoid arachidonoyl glycerol (2-AG) in samples from mNPCs, fully differentiated progeny from mNPCs and mouse HGA cells. Differentiation of NPCs was achieved by growth factor withdrawal and transient addition of fetal bovine serum. After differentiation, we maintained the mNPC progeny in stem cell medium (as used for nondifferentiated mNPCs) and collected the conditioned media. The cell densities in the differentiated and undifferentiated NPCs were equivalent. Using mass-spectrometry, we found that mNPCs contained markedly high amounts of AEA, PEA and OEA, whereas the amounts of these endovanilloids in the differentiated mNPCs and the mouse HGA cells were much lower (**Fig. 2a**). NADA was not detectable in any of the samples (data not shown). We found high concentrations of AEA in the mNPC-CM (**Fig. 2b**), whereas the culture supernatants from the differentiated mNPCs or the HGA cells contained much less AEA, and the concentrations of other lipids were below the detection limit. We observed that the combined application of synthetic AEA, PEA and OEA exerts a cooperative effect on HGA cell death[22], which was blocked by the addition of I-RTX (**Fig. 2c**). The addition of fatty acid amide hydrolase (FAAH), which degrades ethanolamides[23], fully abolished the effect of mNPC-CM (**Fig. 2d**) and of human NPC-CM to induce cell death (data not shown).

We detected only low concentrations of the endocannabinoid 2-AG in mNPCs (**Fig. 2a**; notably, 2-AG concentrations were higher in HGAs than in NPCs). Stimulation of HGAs with the vanilloid NADA induced cell death, and exposure of HGAs to mNPC-CM containing specific cannabinoid receptor antagonists did not blunt the HGA cell death (**Supplementary Figs. 2f**,**g** and **3c**,**d**). Together, these data suggest a role for endovanilloids (rather than endocannabinoids) as mediators of NPC-induced HGA cell death[22]. Next, we used FAAH-deficient (*Faah*$^{-/-}$) mice, which have much higher amounts of endocannabinoids and endovanilloids in the CNS than wild-type mice[24], as a brain tumor model. *Faah*$^{-/-}$ mice are an ideal model to elevate endogenous levels of fatty acid amides. However, the experiments with *Faah*$^{-/-}$ mice foreclosed any comparison to wild-type mice, because, for example, neural stem and immune cells have different activity in *Faah*$^{-/-}$ mice than wild-type mice. Thus, we investigated the effect of TRPV1 signaling on glioma growth by implanting TRPV1-KD or control HGAs into *Faah*$^{-/-}$ mice. We found that implantation of TRPV1-KD tumors resulted in much larger tumors than did implantation of control HGAs in these mice (**Fig. 2e**). These data support our finding from the *in vitro* experiments and show that even greatly elevated concentrations of endogenous endocannabinoids and endovanilloids exert their tumor-suppressive effects exclusively through TRPV1 receptors in our glioma model.

TRPV1 is abundantly expressed in dorsal root ganglion neurons (DRGs)[25], and opening of the TRPV1 channel induces a cation influx, which can be measured, for example, as a rise in the intracellular concentration of free calcium ions. To assess the activity of endovanilloids released from NPCs, we designed a bioassay using DRGs from wild-type and *Trpv1*$^{-/-}$ mice[26]. We stimulated the DRGs from both groups with mNPC-CM and measured the responses using Fura-2–based calcium imaging. We observed that 5.4% of the wild-type DRGs responded to both an initial stimulation with NPC-CM and to a subsequent stimulation with the selective TRPV1 agonist

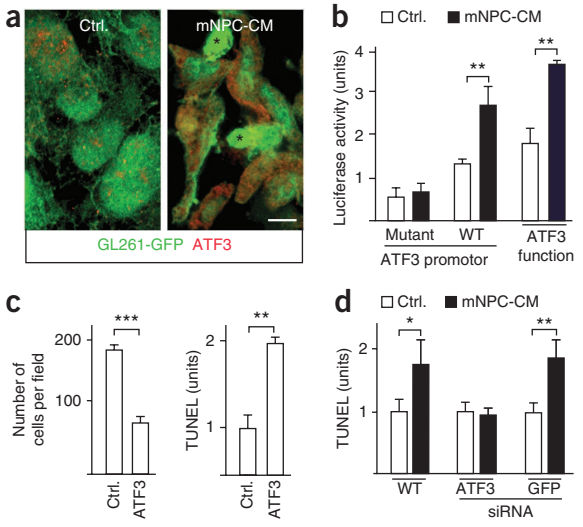

Figure 3 TRPV1 agonists released by NPCs trigger the ATF3 pathway in HGAs. (**a**) ATF3 expression in HGAs (GL261 cells expressing GFP, GL261-GFP) exposed to nonconditioned medium (Ctrl.) or mNPC-CM; notably, the cell morphology changed after exposure to NPC-CM, and the small and rounded GL261 cells (asterisk) seem damaged. Scale bar, 10 μm. (**b**) A wild-type form of the *ATF3* gene promoter (WT) was activated in GL261 cells after stimulation with NPC-CM, whereas a mutant control of the *ATF3* gene promoter (mutant) was not. A gene promoter with an ATF3 binding site (ATF3 function) is also induced after stimulation with mNPC-CM. (**c**) Overexpression of ATF3 reduced GL261 cell density and induced DNA fragmentation (determined by TUNEL) as compared to GL261 cells expressing empty vector (control). (**d**) siRNA for ATF3 prevents mNPC-CM–induced nuclear strand breaks in GL261 HGA cells. All data are mean ± s.d. $*P < 0.05$, $**P < 0.005$, $***P < 0.001$ by Student's *t* test.

capsaicin. Only 0.85% of wild-type DRGs responded to initial stimulation with NPC-CM alone but not to the subsequent stimulation with capsaicin. In *Trpv1*$^{-/-}$ mice, only 0.91% of the DRGs responded to mNPC-CM, which would suggest that TRPV1 is required for the majority of the responses to mNPC-CM observed in the wild-type DRG neurons (**Supplementary Fig. 4a**). In addition, RT-PCR analysis of cultured mNPCs, their differentiated progeny and whole-brain extracts revealed that mNPCs express the major receptors and metabolic enzymes of the endovanilloid and endocannabinoid pathways (**Supplementary Fig. 4b**). These data support the view that endovanilloids are major constituents of mNPC-CM and that endovanilloids are released from NPCs in physiologically relevant concentrations.

Furthermore, mNPC-CM stimulated TRPV1-mediated Ca^{2+} responses in primary human GBM cultures and in human, rat and mouse HGA cell lines (**Fig. 2f** and **Supplementary Fig. 4c**). By performing pharmacological experiments and immunoelectron microscopy, we observed that TRPV1 in the GL261 HGAs was ectopically expressed in the endoplasmic reticulum (ER; **Supplementary Fig. 5b–e**). It has been previously described that TRPV1 in the ER has a lower sensitivity for capsaicin than TRPV1 located in the plasma membrane[16,27]. We also found a lower sensitivity to capsaicin in our experiments (**Supplementary Fig. 4c).**

TRPV1 induces cell death through ER stress

We next investigated the gene expression pattern in mouse tumor cells after incubation with nonconditioned medium (controls) or with mNPC-CM by microarrays (GSE37671). We found that ER stress genes, such as the activating transcription factor-3 gene (*ATF3*), were robustly upregulated in mouse HGA cells treated with mNPC-CM compared to controls. Immunocytochemical labeling and reporter gene assays in GL261 cells treated with mNPC-CM showed that the expression of ATF3 was higher in both the cytoplasm and nucleus of these cells than in controls and that mNPC-CM activates an *ATF3*-responsive element in a gene promoter (**Fig. 3a**,**b**). Forced expression of ATF3 reduced the number of GL261 cells in culture and increased the number of TUNEL^{+} tumor cells (**Fig. 3c**). Notably, siRNA-mediated downregulation of ATF3 expression (**Supplementary Fig. 6a**) in mouse HGA cells prevented the tumor cell death induced by mNPC-CM (**Fig. 3d**). Therefore, ATF3 is necessary and sufficient for mediating the HGA cell death induced by mNPC-CM. Administering the TRPV1 antagonist CZP blocked the mNPC-CM–induced activation of the ATF3-dependent ER stress pathway in mouse HGAs (**Supplementary Fig. 6b**,**c**).

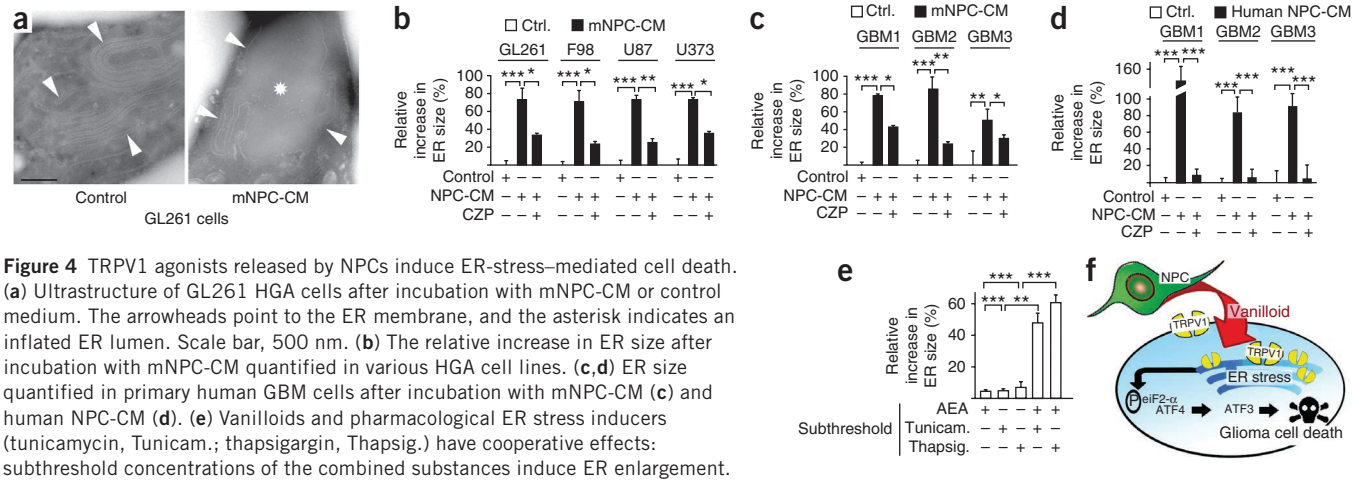

Figure 4 TRPV1 agonists released by NPCs induce ER-stress–mediated cell death. (**a**) Ultrastructure of GL261 HGA cells after incubation with mNPC-CM or control medium. The arrowheads point to the ER membrane, and the asterisk indicates an inflated ER lumen. Scale bar, 500 nm. (**b**) The relative increase in ER size after incubation with mNPC-CM quantified in various HGA cell lines. (**c**,**d**) ER size quantified in primary human GBM cells after incubation with mNPC-CM (**c**) and human NPC-CM (**d**). (**e**) Vanilloids and pharmacological ER stress inducers (tunicamycin, Tunicam.; thapsigargin, Thapsig.) have cooperative effects: subthreshold concentrations of the combined substances induce ER enlargement. (**f**) Illustration of NPCs constitutively releasing endovanilloids (fatty acid ethanolamides such as AEA, PEA and OEA), which traverse the plasma membrane of HGAs and stimulate TRPV1 by docking to an intracellular receptor binding site. NPC-induced TRPV1 activation (mainly located in the ER; **Supplementary Fig. 5**) triggers the ATF3-dependent ER stress pathway in HGAs, which includes activation (phosphorylation, indicated by the P within a circle) of eukaryotic initiation factor 2 α (eiF2-α) and ATF4 (ref. 28; **Supplementary Fig. 6**). Increased expression of ATF3 is necessary and sufficient to mediate HGA cell death. All data are mean ± s.d. $*P < 0.05$, $**P < 0.005$, $***P < 0.001$ by Student's *t* test.

Electron microscopy revealed that GL261 cells treated with mNPC-CM had an enlarged ER as compared to controls (**Fig. 4a** and **Supplementary Fig. 6d**), which is a morphological hallmark of ER stress[28]. We quantified the effect of mNPC-CM (with or without the addition of CZP) on the ER in primary human GBM and in human, rat and mouse HGA cell lines using ER-tracker (**Fig. 4b**,**c**). We then determined the effect of human NPC-CM on ER size in primary human GBMs (**Fig. 4d**). In all HGA cells studied, we detected a very robust increase in ER size after stimulation with human or mouse NPC-CM, which was always attenuated by the addition of CZP (**Fig. 4b–d** and **Supplementary Fig. 7**). Additionally, we used synthetic AEA and inducers of ER stress, such as tunicamycin or thapsigargin[29], at concentrations that were below the threshold for ER stress induction when applied alone. We found that the simultaneous application of AEA and either tunicamycin or thapsigargin led to strong increases in ER size in GL261 cells (**Fig. 4e**). The combined substances had a clear cooperative effect on the rise in ER size, confirming that vanilloid-induced signaling and ER stress are part of the same signal transduction pathway in HGA cells. These data show that human and mouse NPC-derived endovanilloids induce HGA cell death through the ER stress pathway (**Fig. 4f**).

Age dependency of NPC-induced tumor suppression

To investigate whether NPC-derived endovanilloids can suppress HGAs *in vivo*, we performed orthotopic implantation of HGAs into nestin-GFP mice of different ages. Implantation of GL261 cells (TRPV1-KD or controls, which express a nontargeting shRNA) into young (30-day-old) mice resulted in the association of many endogenous NPCs to the tumor[8,9,17] (**Fig. 5a**). Nestin-GFP$^+$ NPCs accumulated at GL261 control HGAs and TRPV1-KD HGAs in equal densities. Notably, we found that young mice injected with TRPV1-KD cells had significantly larger (70%) tumors compared to young mice injected with GL261 control cells (**Fig. 5b**). We found no difference in tumor size in 90-day-old adult mice administered GL261 control cells and those administered TRPV1-KD cells (**Fig. 5b**). In another set of experiments, we used a transgenic mouse model to manipulate the numbers of endogenous NPCs independently of aging. Therefore, we used cyclin D2 knockout (*Ccnd2*$^{-/-}$) mice, which have substantially lower amounts of adult neurogenesis than do wild-type mice[9,30]. In these *Ccnd2*$^{-/-}$ mice and their wild-type littermates, we orthotopically implanted GL261 cells (control or TRPV1-KD) and measured the tumor size 14 d after implantation. We found that the tumor size in the wild-type mice receiving control HGAs was at least 63% smaller than the tumors in the wild-type mice receiving TRPV1-KD tumor cells or *Ccnd2*$^{-/-}$ mice receiving either control HGAs or TRPV1-KD tumor cells (**Fig. 5c**). We then measured HGA cell death *in vivo* by systemically delivering propidium iodide (**Fig. 5d**)[31]. We noted that TRPV1-KD HGAs had much lower levels of HGA cell death than control HGAs.

In another set of experiments, we tested the effect of endovanilloids released from NPCs on the overall survival of a cohort of wild-type mice with HGAs. First, we orthotopically implanted control or TRPV1-KD GL261 cells into young mice and compared the cumulative survival times of the two groups. We observed that young wild-type tumor-bearing mice (**Fig. 5e**) had a significantly longer survival time after implantation than the older mice. However, when we

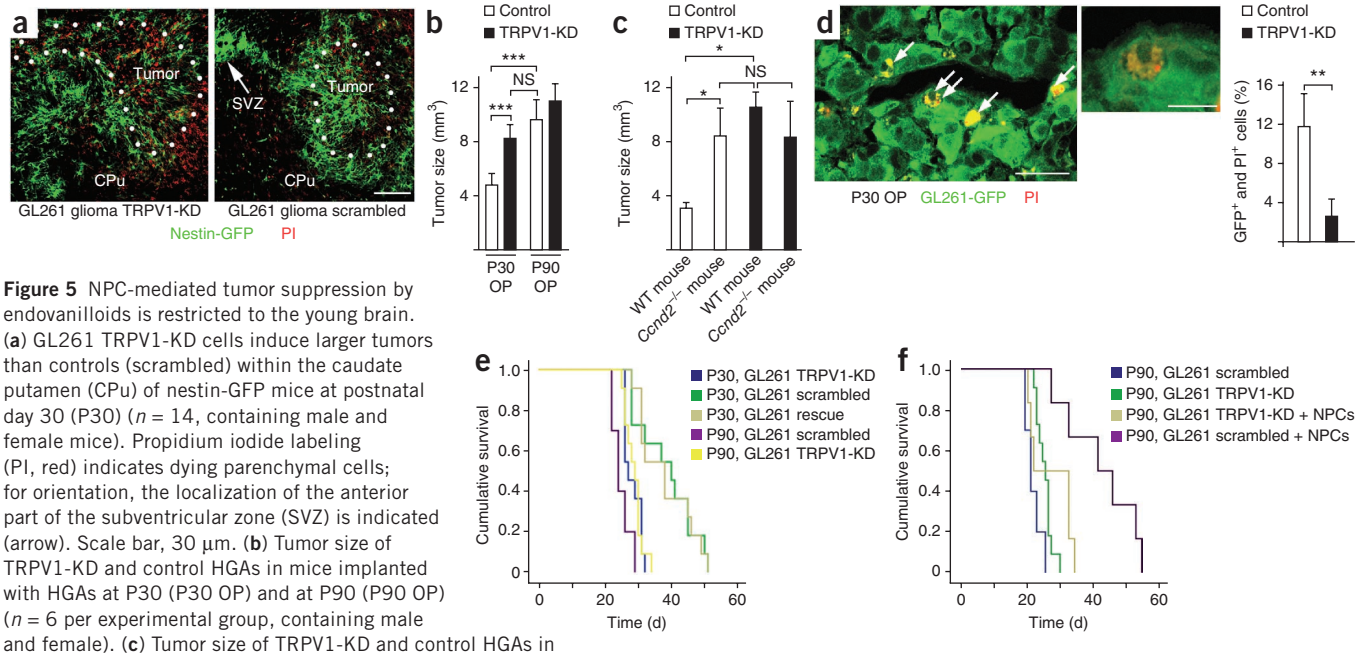

Figure 5 NPC-mediated tumor suppression by endovanilloids is restricted to the young brain. (**a**) GL261 TRPV1-KD cells induce larger tumors than controls (scrambled) within the caudate putamen (CPu) of nestin-GFP mice at postnatal day 30 (P30) ($n = 14$, containing male and female mice). Propidium iodide labeling (PI, red) indicates dying parenchymal cells; for orientation, the localization of the anterior part of the subventricular zone (SVZ) is indicated (arrow). Scale bar, 30 µm. (**b**) Tumor size of TRPV1-KD and control HGAs in mice implanted with HGAs at P30 (P30 OP) and at P90 (P90 OP) ($n = 6$ per experimental group, containing male and female). (**c**) Tumor size of TRPV1-KD and control HGAs in wild-type or *Ccnd2*$^{-/-}$ mice implanted with HGAs at P30; *Ccnd2*$^{-/-}$ mice have reduced neurogenesis ($n = 4$ mice per experimental group, containing male and female). (**d**) Nuclear propidium iodide labeling indicates dying GL261-GFP cells (arrows), and a single PI$^+$ tumor cell is magnified (double arrows) in the image on the right. Quantification of propidium-iodide–labeled (dying) tumor cells. Implantation of TRPV1-KD tumors led to less HGA cell death than implantation of wild-type tumors ($n = 14$ mice, male and female). Scale bar, left, 30 µm; right, 10 µm. (**e**,**f**) The proportion of mice (P30 or P90) surviving HGAs, that is, inoculation with control (scrambled or rescue) or TRPV1-KD GL261 cells. Mice implanted at P30 outlive mice implanted at P90, unless the mice implanted at P30 were given TRPV1-KD tumor cells ($n \geq 10$ mice per group, male and female; **e**). Implantation of P90 mice with both NPCs and control HGAs (scrambled) improves survival but co-injection of NPCs with TRPV1-KD HGAs does not ($n \geq 6$ mice per group, male and female; **f**). All data are mean ± s.d. $^*P < 0.05$, $^{**}P < 0.005$, $^{***}P < 0.001$, NS, not significant by Student's *t* test. In **e** and **f**, survival was statistically significantly different, with $P < 0.001$: in **e**, this comparison was between the 'P30, GL261-scrambled' or 'P30, GL261-rescue' group and all other groups, and in **f**, this comparison was between the 'P90, GL261-scrambled + NPCs' group and all other groups.

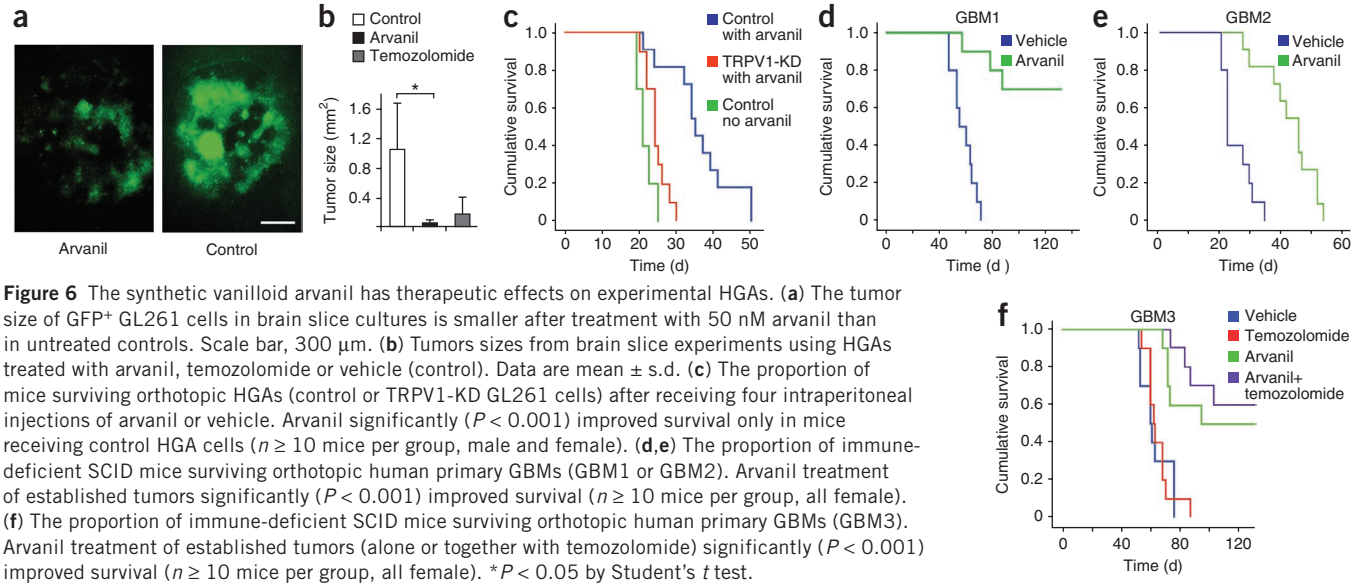

Figure 6 The synthetic vanilloid arvanil has therapeutic effects on experimental HGAs. (**a**) The tumor size of GFP$^+$ GL261 cells in brain slice cultures is smaller after treatment with 50 nM arvanil than in untreated controls. Scale bar, 300 μm. (**b**) Tumors sizes from brain slice experiments using HGAs treated with arvanil, temozolomide or vehicle (control). Data are mean ± s.d. (**c**) The proportion of mice surviving orthotopic HGAs (control or TRPV1-KD GL261 cells) after receiving four intraperitoneal injections of arvanil or vehicle. Arvanil significantly ($P < 0.001$) improved survival only in mice receiving control HGA cells ($n \geq 10$ mice per group, male and female). (**d**,**e**) The proportion of immune-deficient SCID mice surviving orthotopic human primary GBMs (GBM1 or GBM2). Arvanil treatment of established tumors significantly ($P < 0.001$) improved survival ($n \geq 10$ mice per group, all female). (**f**) The proportion of immune-deficient SCID mice surviving orthotopic human primary GBMs (GBM3). Arvanil treatment of established tumors (alone or together with temozolomide) significantly ($P < 0.001$) improved survival ($n \geq 10$ mice per group, all female). *$P < 0.05$ by Student's *t* test.

implanted young mice with TRPV1-KD HGA cells they survived, on average, the same amount of time as older mice. These data show that younger mice have an intrinsic protective mechanism against HGAs that is dependent on endovanilloid signaling. In a second study, we investigated whether the survival-promoting effect that we observed could be attributed specifically to NPCs. Therefore, we implanted adult mice with exogenously cultivated NPCs and control HGAs or TRPV1-KD tumor cells (**Fig. 5f**). We found that implantation of control HGAs always generated tumors but that co-implantation of mNPCs together with HGAs prolonged survival (**Fig. 5e**,**f**; $P < 0.001$). We also found that the survival-promoting effect of NPCs in adult mice was absent after implantation with TRPV1-KD cells (**Fig. 5f**).

Our data suggest that NPCs release endovanilloids *in vivo* in a way similar to NPCs *in vitro*. Consistently, the extent of the NPC-mediated antitumor response depended on the amount of adult neurogenesis.

Synthetic vanilloids as therapeutics for HGAs

We next investigated the therapeutic potential of the synthetic, non-pungent, blood-brain-barrier–permeable vanilloid arvanil[32,33]. We allowed control HGAs to develop for 5 d in organotypic brain slice cultures obtained from wild-type mice. The addition of temozolomide[34] (200 μM, which is the current standard of care for the treatment of patients with GBM) or arvanil (50 nM) strongly reduced the size of the HGAs as compared to vehicle-treated controls (**Fig. 6a**,**b**). Furthermore, arvanil induced a TRPV1-dependent Ca^{2+} signal and TRPV1-dependent cell death in the HGAs (**Supplementary Fig. 8**). In further experiments, we orthotopically implanted TRPV1-KD or control HGAs into wild-type mice and treated both groups with arvanil as described above. We compared the survival of these arvanil-treated mice to a cohort of mice receiving control HGA cells and no arvanil treatment. We found that the mice receiving the control HGAs plus arvanil had significantly longer survival time than the mice receiving TRPV1-KD tumor cells plus arvanil (**Fig. 6c**; $P < 0.001$) or control tumors without arvanil. These data indicate that arvanil elicits its therapeutic effect as a TRPV1 agonist. To determine whether arvanil would also lead to longer survival in other HGA models, we implanted primary human GBM cells (GBM1 and GBM2) into severe combined immunodeficient (SCID) mice. At 1 week after implantation, we examined the tumor development in the mice and administered arvanil (a total of four intraperitoneal injections of 1 mg kg^{-1} body weight each) or vehicle. Treatment with arvanil substantially prolonged survival as compared to treatment with vehicle (**Fig. 6d–f**; $P < 0.001$). We then compared the effects of the application of arvanil and temozolomide (alone and in combination) on survival after implantation of a third primary human HGA culture (GBM3) in immune deficient (SCID) mice. We found that arvanil prolonged survival in a cohort of SCID mice that received GBM3 cells that did not respond to temozolomide (given once daily for 5 d at 100 mg kg^{-1} body weight (ref. 35); **Fig. 6f**; $P < 0.001$). These data show the potential clinical value of an experimental HGA therapy using vanilloids, which may also offer a new therapeutic option for temozolomide-resistant HGAs[36].

DISCUSSION

We have shown that HGAs have high expression of TRPV1 and that TRPV1 stimulation induces tumor cell death. Neural stem and precursor cells home in on HGAs and release antitumorigenic TRPV1 agonists (endovanilloids). Endogenous and exogenous NPCs show extensive tropism for brain tumors[6–10]. However, the number of endogenous NPCs accumulating at HGAs depends on the proliferative activity in the stem cell niche and declines before the onset of adulthood[9]. Hence, the recruitment of large numbers of NPCs to a tumor, and the concomitant antitumorigenic release of endovanilloids, is mostly restricted to the young brain. Additionally, other age-related changes in neural stem cell physiology may also impinge on the ability of NPCs to suppress tumors[37,38].

We show here that NPCs are a primary source of endogenous TRPV1 and cannabinoid receptor agonists such as AEA[15,39]. This finding was supported by our detection of high amounts of AEA and related acylethanolamides in undifferentiated NPCs, as well as our findings that factors released by NPCs evoke TRPV1-dependent Ca^{2+} responses in DRGs and HGAs, that the tumor-suppressive effect of NPC-CM is lost after the addition of FAAH and that NPC-induced HGA cell death is dependent on TRPV1 *in vitro* and *in vivo*. These data are in agreement with previous reports indicating that synthetic AEA induces HGA cell death[40].

A role for TRP channels in tumor suppression was previously suggested by us and others[41–45], but the present study is the first, to our knowledge, to identify NPCs as a cellular source for

tumor-suppressive endovanilloids and uncover the role of TRPV1 agonists and modulators released by NPCs on HGA cell death. Overall, our study suggests that endovanilloids are intrinsic tumor suppressors in the brain and that synthetic vanilloid compounds may have clinical potential for the treatment of brain tumors.

METHODS

Methods and any associated references are available in the online version of the paper.

Accession codes. Microarray data are deposited in Gene Expression Omnibus under the accession code GSE37671.

Note: Supplementary information is available in the online version of the paper.

ACKNOWLEDGMENTS

We thank G. Gargiulo, O. Daumke and J. Kurreck for discussion of the manuscript, S. Kitajima (Medical Research Institute, Tokyo Medical and Dental University, Tokyo, Japan) for ATF3 constructs and L. Kaczmarek and M. Szymanska (Nencki Institute, Warsaw, Poland) for providing *Ccnd2*$^{-/-}$ mice. We acknowledge funding from the Helios Clinics (HeFoFö-ID1148) and the US National Institutes of Health (DA-009789 to V.D.M.).

AUTHOR CONTRIBUTIONS

S.P., R.I., A.L., L.D.P., U.G. and S.R.C. designed and conducted the experiments, and interpreted the data. K.S., J.K., E.S.J.S., P.W., B.P., U.A.N., V.M., B.F.C., S.M., V.D.M., J.-H.W., G.D. and L.C. contributed to manuscript preparation. G.R.L., V.D.M. and H.K. designed the experiments, supervised the project, interpreted the data and contributed to manuscript preparation. M.S. performed brain tumor resections and provided tumor samples. M.S. and R.G. designed and conducted the experiments, supervised the project, interpreted the data and prepared the manuscript.

COMPETING FINANCIAL INTERESTS

The authors declare no competing financial interests.

Published online at http://www.nature.com/doifinder/10.1038/nm.2827.
Reprints and permissions information is available online at http://www.nature.com/reprints/index.html.

1. Sanai, N., Alvarez-Buylla, A. & Berger, M.S. Neural stem cells and the origin of gliomas. *N. Engl. J. Med.* **353**, 811–822 (2005).
2. Ohgaki, H. & Kleihues, P. Epidemiology and etiology of gliomas. *Acta Neuropathol.* **109**, 93–108 (2005).
3. Ohgaki, H. & Kleihues, P. Genetic pathways to primary and secondary glioblastoma. *Am. J. Pathol.* **170**, 1445–1453 (2007).
4. Knoth, R. *et al.* Murine features of neurogenesis in the human hippocampus across the lifespan from 0 to 100 years. *PLoS ONE* **5**, e8809 (2010).
5. Leuner, B., Kozorovitskiy, Y., Gross, C.G. & Gould, E. Diminished adult neurogenesis in the marmoset brain precedes old age. *Proc. Natl. Acad. Sci. USA* **104**, 17169–17173 (2007).
6. Assanah, M. *et al.* Glial progenitors in adult white matter are driven to form malignant gliomas by platelet-derived growth factor–expressing retroviruses. *J. Neurosci.* **26**, 6781–6790 (2006).
7. Assanah, M.C. *et al.* PDGF stimulates the massive expansion of glial progenitors in the neonatal forebrain. *Glia* 1835–1847 (2009).
8. Glass, R. *et al.* Glioblastoma-induced attraction of endogenous neural precursor cells is associated with improved survival. *J. Neurosci.* **25**, 2637–2646 (2005).
9. Walzlein, J.H. *et al.* The antitumorigenic response of neural precursors depends on subventricular proliferation and age. *Stem Cells* **26**, 2945–2954 (2008).
10. Aboody, K.S. *et al.* Neural stem cells display extensive tropism for pathology in adult brain: evidence from intracranial gliomas. *Proc. Natl. Acad. Sci. USA* **97**, 12846–12851 (2000).
11. Suzuki, T. *et al.* Inhibition of glioma cell proliferation by neural stem cell factor. *J. Neurooncol.* **74**, 233–239 (2005).
12. Staflin, K. *et al.* Neural progenitor cell lines inhibit rat tumor growth *in vivo*. *Cancer Res.* **64**, 5347–5354 (2004).
13. Staflin, K., Zuchner, T., Honeth, G., Darabi, A. & Lundberg, C. Identification of proteins involved in neural progenitor cell targeting of gliomas. *BMC Cancer* **9**, 206 (2009).
14. Starowicz, K., Nigam, S. & Di Marzo, V. Biochemistry and pharmacology of endovanilloids. *Pharmacol. Ther.* **114**, 13–33 (2007).
15. Tóth, A., Blumberg, P.M. & Boczan, J. Anandamide and the vanilloid receptor (TRPV1). *Vitam. Horm.* **81**, 389–419 (2009).
16. Szallasi, A., Cortright, D.N., Blum, C.A. & Eid, S.R. The vanilloid receptor TRPV1: 10 years from channel cloning to antagonist proof-of-concept. *Nat. Rev. Drug Discov.* **6**, 357–372 (2007).
17. Chirasani, S.R. *et al.* Bone morphogenetic protein-7 release from endogenous neural precursor cells suppresses the tumourigenicity of stem-like glioblastoma cells. *Brain* **133**, 1961–1972 (2010).
18. Yamaguchi, M., Saito, H., Suzuki, M. & Mori, K. Visualization of neurogenesis in the central nervous system using nestin promoter-GFP transgenic mice. *Neuroreport* **11**, 1991–1996 (2000).
19. Zhao, C., Deng, W. & Gage, F.H. Mechanisms and functional implications of adult neurogenesis. *Cell* **132**, 645–660 (2008).
20. Okano, H., Imai, T. & Okabe, M. Musashi: a translational regulator of cell fate. *J. Cell Sci.* **115**, 1355–1359 (2002).
21. Cullen, B.R. Enhancing and confirming the specificity of RNAi experiments. *Nat. Methods* **3**, 677–681 (2006).
22. Lambert, D.M. & Di Marzo, V. The palmitoylethanolamide and oleamide enigmas: are these two fatty acid amides cannabimimetic? *Curr. Med. Chem.* **6**, 757–773 (1999).
23. Ueda, N., Puffenbarger, R.A., Yamamoto, S. & Deutsch, D.G. The fatty acid amide hydrolase (FAAH). *Chem. Phys. Lipids* **108**, 107–121 (2000).
24. Cravatt, B.F. *et al.* Supersensitivity to anandamide and enhanced endogenous cannabinoid signaling in mice lacking fatty acid amide hydrolase. *Proc. Natl. Acad. Sci. USA* **98**, 9371–9376 (2001).
25. Stürzebecher, A.S. *et al.* An *in vivo* tethered toxin approach for the cell-autonomous inactivation of voltage-gated sodium channel currents in nociceptors. *J. Physiol. (Lond.)* **588**, 1695–1707 (2010).
26. Caterina, M.J. *et al.* Impaired nociception and pain sensation in mice lacking the capsaicin receptor. *Science* **288**, 306–313 (2000).
27. Gallego-Sandín, S., Rodriguez-Garcia, A., Alonso, M.T. & Garcia-Sancho, J. The endoplasmic reticulum of dorsal root ganglion neurons contains functional TRPV1 channels. *J. Biol. Chem.* **284**, 32591–32601 (2009).
28. Hori, O. *et al.* Role of Herp in the endoplasmic reticulum stress response. *Genes Cells* **9**, 457–469 (2004).
29. Xu, C., Bailly-Maitre, B. & Reed, J.C. Endoplasmic reticulum stress: cell life and death decisions. *J. Clin. Invest.* **115**, 2656–2664 (2005).
30. Kowalczyk, A. *et al.* The critical role of cyclin D2 in adult neurogenesis. *J. Cell Biol.* **167**, 209–213 (2004).
31. Unal Cevik, I. & Dalkara, T. Intravenously administered propidium iodide labels necrotic cells in the intact mouse brain after injury. *Cell Death Differ.* **10**, 928–929 (2003).
32. Melck, D. *et al.* Unsaturated long-chain N-acyl-vanillyl-amides (N-AVAMs): vanilloid receptor ligands that inhibit anandamide-facilitated transport and bind to CB1 cannabinoid receptors. *Biochem. Biophys. Res. Commun.* **262**, 275–284 (1999).
33. Veldhuis, W.B. *et al.* Neuroprotection by the endogenous cannabinoid anandamide and arvanil against *in vivo* excitotoxicity in the rat: role of vanilloid receptors and lipoxygenases. *J. Neurosci.* **23**, 4127–4133 (2003).
34. Fisher, T. *et al.* Mechanisms operative in the antitumor activity of temozolomide in glioblastoma multiforme. *Cancer J.* **13**, 335–344 (2007).
35. McConville, P. *et al.* Magnetic resonance imaging determination of tumor grade and early response to temozolomide in a genetically engineered mouse model of glioma. *Clin. Cancer Res.* **13**, 2897–2904 (2007).
36. Mrugala, M.M. & Chamberlain, M.C. Mechanisms of disease: temozolomide and glioblastoma–look to the future. *Nat. Clin. Pract. Oncol.* **5**, 476–486 (2008).
37. Conover, J.C. & Shook, B.A. Aging of the subventricular zone neural stem cell niche. *Aging Dis.* **2**, 149–163 (2011).
38. Khan, M.A. & Lie, D.C. MicroRNA—a contributor to age-associated neural stem cell dysfunction? *Aging* **3**, 182–183 (2011).
39. Di Marzo, V., Gobbi, G. & Szallasi, A. Brain TRPV1: a depressing TR(i)P down memory lane? *Trends Pharmacol. Sci.* **29**, 594–600 (2008).
40. Maccarrone, M., Lorenzon, T., Bari, M., Melino, G. & Finazzi-Agro, A. Anandamide induces apoptosis in human cells via vanilloid receptors. Evidence for a protective role of cannabinoid receptors. *J. Biol. Chem.* **275**, 31938–31945 (2000).
41. Izzo, A.A. *et al.* Increased endocannabinoid levels reduce the development of precancerous lesions in the mouse colon. *J. Mol. Med.* **86**, 89–98 (2008).
42. Prevarskaya, N., Zhang, L. & Barritt, G. TRP channels in cancer. *Biochim. Biophys. Acta* **1772**, 937–946 (2007).
43. Bode, A.M. *et al.* Transient receptor potential type vanilloid 1 suppresses skin carcinogenesis. *Cancer Res.* **69**, 905–913 (2009).
44. Visnyei, K. *et al.* A molecular screening approach to identify and characterize inhibitors of glioblastoma stem cells. *Mol. Cancer Ther.* **10**, 1818–1828 (2011).
45. Morelli, M.B. *et al.* The Transient Receptor Potential Vanilloid-2 (TRPV2) cation channel impairs glioblastoma stem-like cell proliferation and promotes differentiation. *Int. J. Cancer* published online, doi:10.1002/ijc.27588 (11 April 2012).

ONLINE METHODS

Mice. Mouse experiments were carried out in compliance with the German laws on animal welfare, and the mouse protocols were approved by the Landesamt für Gesundheit und Soziales (LaGeSo) in Berlin. Wild-type C57BL/6 mice, nestin-GFP[18] mice, *Trpv1*$^{-/-}$ mice[26], *Ccnd2*$^{-/-}$ mice[29], *Faah*$^{-/-}$ mice[24] and SCID mice (B6.CB17-*Prkdc*^{SCID}/SzJ, Charles River Breeding Laboratories, Schöneiche, Germany) were all of both sexes and were housed with a 12 h light, 12 h dark cycle and received food *ad libitum*.

SVZ specimens, tumor specimens, GBM complementary DNA (cDNA) arrays and normal brain cDNA arrays. Normal SVZ specimens from human brains were obtained as part of planned resections during anterior temporal lobectomy for the treatment of intractable epilepsy from mesial temporal sclerosis. Tumor samples were obtained from otherwise untreated primary GBMs from patients undergoing planned tumor resections at the Charité University Clinics. We obtained ethical approval for the human studies from the ethics committee of the Charité University clinics (EA112/2001, EA3/023/06 and EA2/101/08). According to German governmental and internal (Charité University) rules and regulations, all patients gave informed consent to use the material for scientific experimentation; cDNA samples and tissue arrays from human brain tumors and from tumor-free brain were obtained from OriGene.

Cell culture. All GBM cells were maintained as previously described for neurospheres[46]. Mouse, rat and human HGA cell lines and 293T cells were obtained from the National Cancer Institute, the Frederick National Laboratory for Cancer Research and from American Type Culture Collection. Mouse NPCs were obtained from the SVZ of wild-type mice; DRG neurons were prepared from both wild-type and *Trpv1*$^{-/-}$ adult mice, as described previously[25].

shRNA experiments. The pLKO.1 shRNA vector was from Bio-Cat. The validity of the shRNA-mediated knockdown was affirmed on the protein level by western blotting and fluorescence-activated cell sorting, as previously described[47], as well as on the functional level (by calcium imaging and cytotoxicity assays). The TRPV1 rescue construct was mutated in the seed region of the shRNA knockdown construct[21].

Cytotoxicity assays. CytoTox-Fluor Cytotoxicity Assays (Promega) were measured (485 nm/520 nm) with the fluorometer (Tecan).

TUNEL assay. TUNEL^{+} cells were quantified using the DELFIA Cell-Based Fragmentation Assay (PerkinElmer).

Measurement of ER size. HGA cells were seeded in poly-L-lysine (PLL)-coated µ-slide 8-well plates and treated with NPC-conditioned medium with or without TRPVI antagonist. The ER stress inducer thapsigargin (30 ng ml^{-1}) was added to the positive control wells for 6 h. For live-cell ER labeling, ER tracker solution (500 nM) was added to the cells for an incubation time of 30 min at 37 °C. Subsequently, the stained cells were fixed with 4% PFA for 15 min at room temperature. The staining was evaluated using a DAPI longpass filter. The relative increase in ER size after incubation with NPC-conditioned medium was quantified by confocal microscopy *z*-stacks (nonconditioned medium was used as the control; incubation with thapsigargin was set as 100%). For antagonist treatment, the cells were preincubated with antagonists for 3 h in control medium. Afterward, the medium was exchanged with medium containing agonist and antagonist.

Microarray analyses. cDNA microarrays[48] were generated using ~20,000 mouse cDNA clones (ArrayTag clone collection) from LION Bioscience, and six arrays were used in total. Image acquisition and data analyses were done as previously described[48].

HPLC and mass spectrometry. Lipids were purified using open-bed chromatography on silica gel, and AEA, 2-AG, PEA, OEA and NADA were analyzed by isotope dilution–liquid chromatography/atmospheric pressure chemical ionization/mass spectrometry[49–51].

Peptides for the development of a selected reaction monitoring (SRM) method were selected. Cells were lysed, digested using protease, purified, separated by HPLC and electrosprayed into the mass spectrometer (AB SCIEX QTRAP 4000). For the data analyses, the MultiQuant (AB SCIEX) and R software packages (http://www.r-project.org/) were used[52].

Calcium measurements. Cells were loaded with Fura-2-acetoxymethyl ester (TEFLabs), excited at 340 nm and 380 nm, and imaged with a 510-nm long-pass filter; the results are presented as the ratio between the emission signals acquired using the two excitation wavelengths.

Real-time PCR. Real-time PCR was performed on the iCycler IQ 5 multicolor real-time detection system (Bio-Rad) using absolute SYBR Green/Fluorescein (Abgene). Oligonucleotides were purchased from Invitrogen.

Western blot. Membranes were incubated with specific antibodies, and western blots were developed using the chemiluminescence method (GE Healthcare).

Tumor implantation. Surgical procedures were performed as previously described[8,9]: anesthetized mice received tumors (2×10^4 HGA cells per 1 µl; this applies to all HGA cells used for *in vivo* experimentation in this study, Gl261, GBM1, GBM2 or GBM3) alone or in combination with exogenously cultivated NPCs (6×10^4 precursor cells in 4 µl).

Immunofluorescence and microscopy. All stainings and microscopies for NPC and HGA markers were carried out as described previously[53].

Electron microscopy. For the ER visualization, ultrathin cryosections (70 nm) of fixed HGA cells were contrasted, stabilized[54] and examined with a Zeiss 910 electron microscope. For immunogold labeling before embedding, HGA cells were fixed in 4% paraformaldehyde and 1% glutaraldehyde and incubated with TRPV1-specific antibody.

Cell counting and unbiased stereology. In every twelfth axial section, we sampled the area that was primarily infiltrated by the tumor in an unbiased approach using the optical fractionator procedure (Stereo Investigator, MicroBrightField Inc.). Tumor volume was quantified according to Cavalieri's principle.

Statistical analyses. Survival statistics were analyzed using MatLab software (Natick, MA). Bar diagrams are shown as means ± s.d. Comparisons among the groups were performed with the Student's *t* test, Fisher's exact test and the Wilcoxon rank test (as indicated).

46. Lee, J. *et al.* Tumor stem cells derived from glioblastomas cultured in bFGF and EGF more closely mirror the phenotype and genotype of primary tumors than do serum-cultured cell lines. *Cancer Cell* **9**, 391–403 (2006).
47. Grünweller, A. *et al.* Comparison of different antisense strategies in mammalian cells using locked nucleic acids, 2′-O-methyl RNA, phosphorothioates and small interfering RNA. *Nucleic Acids Res.* **31**, 3185–3193 (2003).
48. Gurok, U. *et al.* Gene expression changes in the course of neural progenitor cell differentiation. *J. Neurosci.* **24**, 5982–6002 (2004).
49. Devane, W.A. *et al.* Isolation and structure of a brain constituent that binds to the cannabinoid receptor. *Science* **258**, 1946–1949 (1992).
50. Bisogno, T., Maurelli, S., Melck, D., De Petrocellis, L. & Di Marzo, V. Biosynthesis, uptake, and degradation of anandamide and palmitoylethanolamide in leukocytes. *J. Biol. Chem.* **272**, 3315–3323 (1997).
51. Marsicano, G. *et al.* The endogenous cannabinoid system controls extinction of aversive memories. *Nature* **418**, 530–534 (2002).
52. de Godoy, L.M. *et al.* Comprehensive mass-spectrometry–based proteome quantification of haploid versus diploid yeast. *Nature* **455**, 1251–1254 (2008).
53. Kempermann, G., Gast, D., Kronenberg, G., Yamaguchi, M. & Gage, F.H. Early determination and long-term persistence of adult-generated new neurons in the hippocampus of mice. *Development* **130**, 391–399 (2003).
54. Reimer, T.A. *et al.* Reevaluation of the 22–1-1 antibody and its putative antigen, EBAG9/RCAS1, as a tumor marker. *BMC Cancer* **5**, 47 (2005).